S. S. Zhou, X. Q. Liu*, Z. L. Liu, Z. G. Hou and Q. C. Tian

Dynamic Recrystallization Behavior of Vanadium Microalloyed Cryogenic Fine Grain Structural Steel Pipe at High Strain Rate

DOI 10.1515/htmp-2016-0063
Received March 22, 2016; accepted September 2, 2016

Abstract: Dynamic recrystallization (DRX) behavior of a vanadium microalloyed steel pipe was systematically investigated at temperatures range of 850–1,200 °C and a strain rate of 5 s^{-1} on a Gleeble-3800 thermo-simulation machine. Constitutive equation was obtained by characteristic points of DRX which derived from the strain hardening rate and stress curves. DRX kinetics model was established for determining the recrystallization volume fraction (X). Effect of dynamic precipitation of V(C, N) imposed on DRX at temperatures from 850–1,000 °C was analyzed. Results show that true stress-strain curves exhibited no clearly defined stress peaks with typical dynamic recovery behavior. X increased from 43.9 % to 100 % with increasing deformation temperature, which was in reasonable agreement with the observation of microstructure. Moreover, the calculation pinning force of V(C, N) precipitates was weaker than the recrystallization driving force, revealing that V(C, N) precipitates could effectively retard rather than prevent the progress of DRX.

Keywords: dynamic recrystallization behavior, vanadium microalloyed, cryogenic fine grain structural steel pipe, high strain rate

Introduction

S(355–460)NL vanadium microalloyed fine grain structural steel pipes have been developed based on the criterion of EN10210, enhanced by means of V mircroalloying, controlled rolling and cooling technology, exhibiting excellent mechanical properties at normalized condition and guaranteed the low temperature impact toughness at –20~–50 °C [1]. As for the excellent cryogenic toughness and security, S(355–460)NL structural steel plays a very important role in alpine region, including construction, bridge, petroleum pipeline and other fields [2, 3]. Previously, most studies concentrate on the effect of heat-treating process imposed on cryogenic toughness and corrosion behavior of vanadium microalloyed fine grain structural steel pipes [4, 5]. However, dynamic recrystallization behavior of this material has been less investigated.

In the rolling deformation process of steel pipe which performed at high temperature and strain rate, DRX plays a major role in reducing the flow stress and controlling the final grain size, which directly influences the final mechanical properties [6]. Strain rate of the skew rolling process of steel pipe is about 4~6 s^{-1} and true stress-strain curves have the characteristics of dynamic recovery type while strain rate exceeds 1 s^{-1} [7–9]. The presence of stress peaks in constant strain rate flow curves is traditionally identified as the sole reliable indication of the initiation of DRX [10]. Nevertheless, it was demonstrated that materials such as Nb microalloyed low carbon and austentic stainless steels, presented recrystallization grains with no obvious peak characteristic in their rheological curves [11–13]. Therefore, it is essential to understand the DRX behavior at high strain rate.

The microalloying elements, especially Nb, Ti as well as V, imposed a strong solute drag effect on solution and produce the pinning force by forming fine precipitates. Both improvements play an effective role through retarding the recrystallization and then help inhibit the growth of recrystallization grains [14]. There have already been many researches on the deformation behavior of Nb and Ti microalloyed steel [15, 16]. However, the influence of strain induced V(C, N) precipitation behavior during hot deformation on the DRX is still not clear. Medina et al. [17] and Wei et al. [18] considered that the addition of V in the microalloyed steels exhibited no effects on the DRX. In contrast, Wu et al. [19] calculated the pinning force of V(C, N) precipitates in a Mn-Cu-V weathering steel, discovering that dynamic precipitation could retard the progress of dynamic recrystallization. Furthermore, the most

***Corresponding author: X. Q. Liu,** College of Materials Science and Engineering, Nanjing University of Aeronautics and Astronautics, Nanjing 210016, China, E-mail: liuxiqin@nuaa.edu.cn
S. S. Zhou, Z. L. Liu, Z. G. Hou, College of Materials Science and Engineering, Nanjing University of Aeronautics and Astronautics, Nanjing 210016, China
Q. C. Tian, Baoshan Iron & Steel Co, Ltd, Shanghai 201900,China

recent work in the calculation of pinning force focused on low strain rate at different true strain [19, 20].

Therefore, this paper aims to research on the dynamic recrystallization and dynamic precipitation behaviors of a vanadium microalloyed steel pipe over the temperature range of 850–1,200 °C and a high strain rate of 5 s^{-1} on a Gleeble-3800 thermo-simulation machine.

Experimental materials and procedures

The materials used in this investigation were vanadium microalloyed cryogenic fine grain hot-rolled steel plate developed by Baoshan Iron & Steel Co, Ltd with chemical composition given in Table 1. Cylindrical samples of Φ 8 mm × 12 mm were cut off from the hot-rolled steel plate, and the hot compression tests were conducted on a Gleeble-3800 thermo-mechanical simulator. To prevent the oxidation of samples in the process of heating and deformation, high purity Argon was used as a protective gas. Simultaneously, graphite powder was also used as a lubricant to reduce the friction between the specimens and the anvils. Samples were reheated in vacuum at the rate of 10 °C/s to 1,250 °C for 5 min, then cooled down to the deformation temperature and held for 1 min. Deformation temperature ranges from 850 to 1,200 °C at an interval of 50 °C and strain rate is 5 s^{-1}. Samples were compressed to a total true stain of 0.9, parts of them were then water quenched immediately to freezing high-temperature microstructure.

Table 1: Chemical composition of vanadium microalloyed fine grain structural steel under investigation (in mass %).

C	Si	Mn	S	P	N	V	Cr + Ni + Cu	Fe
0.19	0.25	1.5	0.003	0.008	0.008	0.14	0.43	Bal.

The deformed samples were sectioned parallel to the longitudinal axis. A saturated aqueous picric acid solution was polished to reveal the original austenite grain boundaries. Hot deformation microstructure was observed on a XJ-16A optical microscope and average grain size were measured by the intersection point method according to the criterion of GB/T6394-2002. In order to verify the strain-induced V(C, N) precipitation behavior at high strain rate, samples deformed at temperatures from 850 to 1,000 °C were thinned by an electro twin polishing technique using a solution consisting of 95 % acetic acid and 5 % perchloric acid, and then were observed by transmission electron microscopy (TEM, FEI G^2 F20).

Results and discussion

Hot deformation true stress-strain curves

Figure 1 shows the true stress-strain (*σ*-*ε*) curves of vanadium microalloyed cryogenic fine grain structural steel pipe deformed at the strain rate of 5 s^{-1} with temperature ranging from 850 to 1,200 °C. The *σ*-*ε* curves exhibit no clearly defined stress peaks with typical dynamic recovery behavior and the flow stress increases gradually with the decrease in deformation temperature. In the initial stage of hot deformation, *σ*-*ε* curve increases rapidly, which is mainly attributed to the work hardening effect resulting from lattice distortion and the pile-up of dislocations during deformation. As the true strain reaching a certain degree, the increasing rate of *σ*-*ε* curve decreases due to the occurrence of dynamic recovery (DRV), which is caused by the annihilation or rearrangement of partial dislocations through sliding and climbing. After that, *σ*-*ε* curve becomes smooth, indicating the presence of the dynamic equilibrium in increment and decrement of the dislocations. As for no clearly defined stress peaks in *σ*-*ε* curves, the main reason is that higher strain rate provides shorter time for energy accumulation and

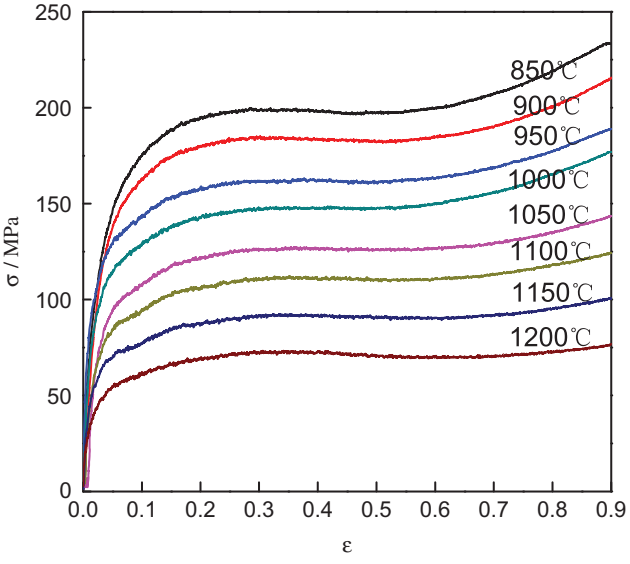

Figure 1: True stress-strain curves of samples deformed under temperatures from 850 °C to 1,200 °C

lower mobility's at boundaries for the nucleation of DRX, the dynamic softening effect can hardly exceed work hardening effect [21]. Furthermore, the driving force of atomic diffusion and dislocation vacancies for cross slip increases with the increasing temperature, which enhances the dynamic softening behavior and leads to the decrease in flow stress [19].

Hot deformation microstructure

Figure 2 shows the microstructure of vanadium microalloyed cryogenic fine grain structural steel pipe deformed with temperature ranging from 850 °C to 1,200 °C. Different degree of DRX occurs in all compression deformation samples, which indicates that the presence of the stress peaks is

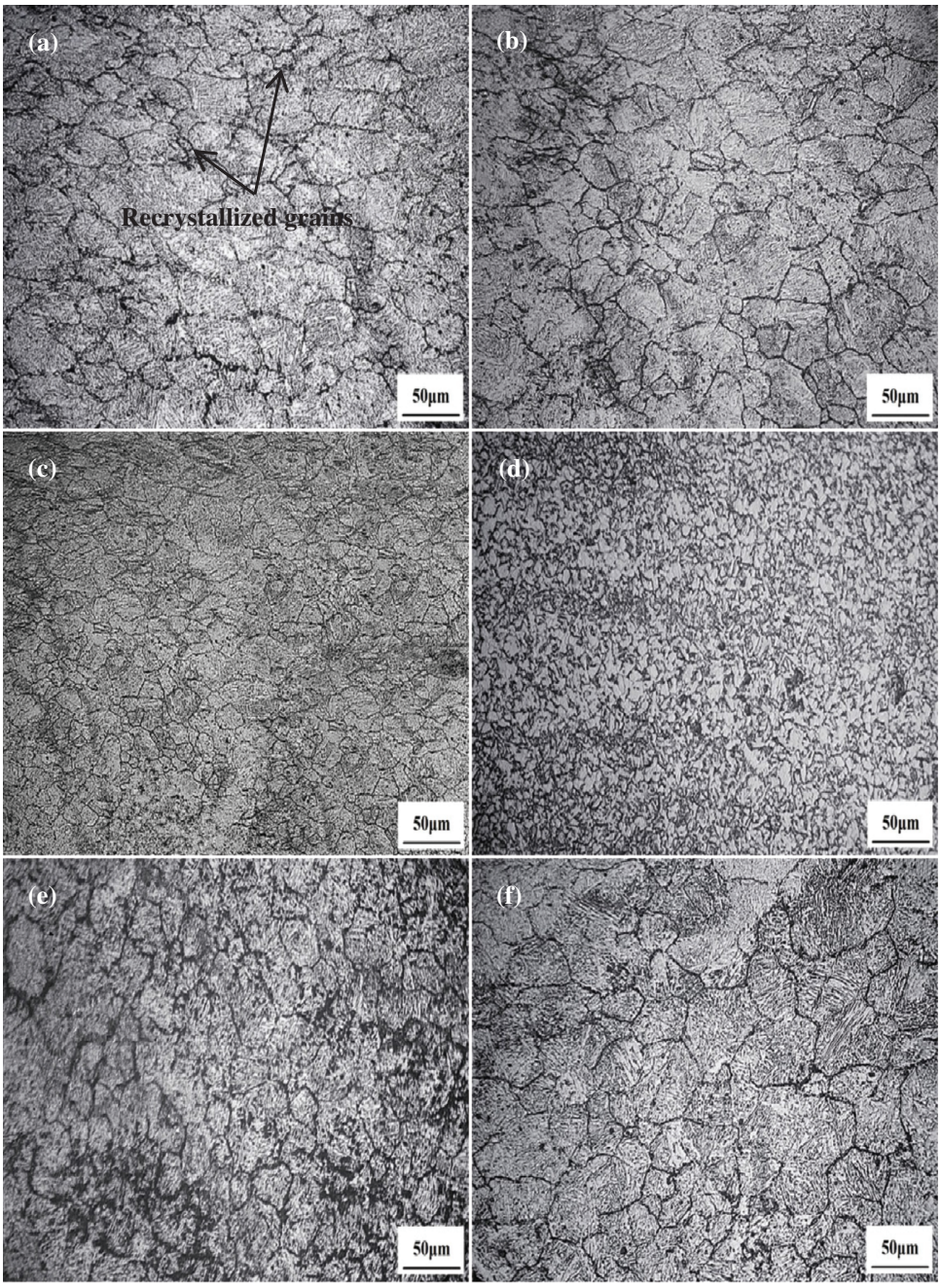

Figure 2: The compression deformation microstructure of samples under temperatures of 850–1,200 °C (a) 850 °C (b) 900 °C (c) 950 °C (d) 1,050 °C (e) 1,100 °C (f) 1,200 °C.

with no respect to the occurrence of DRX. It can be seen in Figure 2(a) that a small amount of fine near-equiaxed DRX grains exist in the contact area of several coarse original austenitic grains. With the increasing deformation temperature (Figure 2(b) and (c)), the prior austenitic grains are gradually replaced by recrystallization grains and the average grain size decreases continuously. As the deformation temperature increased to 1,050 °C (Figure 2(d)), the mircrostructure consists of completed recrystallization grains with a mean grain size of 9 μm. With further increased in the deformation temperature (Figure 2(e) and (f)), the DRX grains begin coarsening.

Constitutive analysis

For further investigating the DRX behavior of the experimental steel, it is essential to determine DRX characteristic points based on the dynamic recovery type true stress-strain curves, including critical stress (strain) and peak stress (strain). However, characteristic points are difficult to be determined accurately by microstructure observation. To solve the problem, Najafizadeh et al. [22] have already achieved the strain hardening rate θ ($\theta = d\sigma/d\varepsilon$) and true stress σ curve by using three polynomial nonlinear fitting and determined the DRX characteristic points. However, the method mentioned above cannot ensure the accuracy of the θ-σ curve at high data fluctuation. In this article, θ-σ curves were accurately determined by nine polynomial nonlinear fitting, as shown in Figure 3. θ-σ curve can be divided into four stages. In stage I, strain hardening rate decreases quickly with the increasing flow stress; Subsequently, dislocations form tangles and polygonize into subgrain boundaries, which slowed the rate of dynamic recovery, then the slope of θ-σ curve decreases and the curve enters stage II [23, 24]; When the flow stress reaches the critical value, the DRX is expected to take place with an inflection point appearing in θ-σ curve, then the strain hardening rate decreases quickly and the curve comes into stage III; The stage IV starts in the time that the strain hardening rate drops to a value below zero. According to the approach proposed by Jonas et al. [18], the point at which the work hardening rate equals zero ($\theta = 0$) in θ-σ curve represents the peak stress (σ_p). The inflection point of θ-σ curve indicates the critical stress (σ_c) for the initiation of DRX which then can be directly detected from the minimum value of (-dθ/dσ)-σ curve (Figure 4). Values of critical stress (σ_c), peak stress (σ_p), critical strain (ε_c), peak strain (ε_p) and $\varepsilon_c/\varepsilon_p$ are listed in Table 2. It can be seen that σ_c, σ_p, ε_c and ε_p

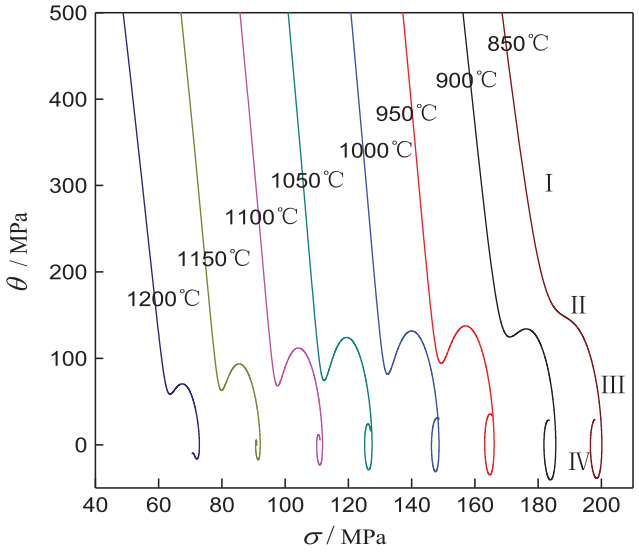

Figure 3: θ-σ curves of samples deformed under temperatures from 850 °C to 1,200 °C.

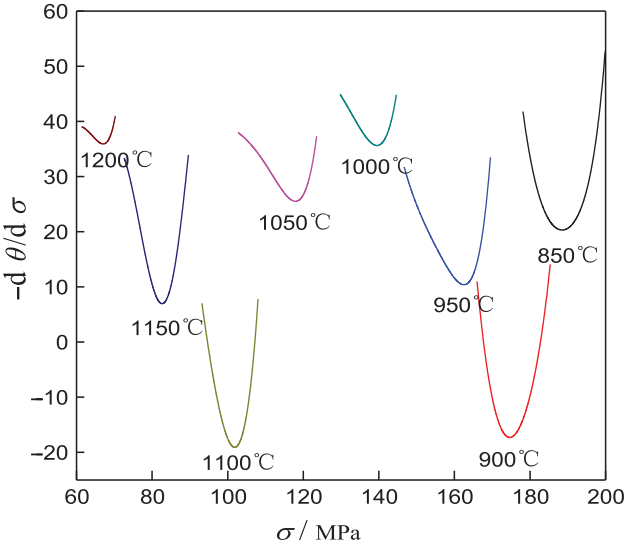

Figure 4: (–dθ/dσ)-σ curves of samples deformed under temperatures from 850 °C to 1,200 °C.

Table 2: Dynamic recrystallization characteristic values deformed under temperatures from 850 °C to 1,200 °C.

T/°C	σ_c	σ_p	ε_c	ε_p	$\varepsilon_c/\varepsilon_p$
850	191.99	199.35	0.17550	0.35948	0.48820
900	176.45	184.44	0.16862	0.34057	0.49511
950	157.09	164.97	0.16325	0.32407	0.50375
1,000	139.18	147.87	0.15698	0.29849	0.52591
1,050	117.26	126.27	0.14819	0.27178	0.54526
1,100	101.68	110.02	0.13721	0.25260	0.54319
1,150	82.26	90.52	0.12883	0.23380	0.55103
1,200	62.43	70.12	0.12080	0.21550	0.56056

increase while $\varepsilon_c/\varepsilon_p$ decreases with decreased deformation temperature. The range of ratio in $\varepsilon_c/\varepsilon_p$ is about 0.48~0.56, closed to the lower limit of the empirical model of Sellars ($\varepsilon_c = (0.6\sim0.85)\varepsilon_p$) [25], which demonstrates the stronger work hardening ability of tested samples at high strain rate.

Flow stress is in closely related to deformation temperature and strain rate, and such relationship can be described by Zener-Hollomon Parameter (Z) in an exponent type constitutive equation [26]:

$$Z = \dot{\varepsilon}\exp(Q/RT) = A\sigma_p{}^n \tag{1}$$

where $\dot{\varepsilon}$ represents the strain rate; Q is the deformation activation energy (kJ/mol); R is the universal gas constant (8.314 J/mol); T is the absolute temperature (K); σ_p is the peak stress (MPa); A and n are material constants.

Taking natural logarithm for both sides of eq. (1):

$$\ln Z = \ln\dot{\varepsilon} + \frac{Q}{RT} = n\ln\sigma_p + \ln A \tag{2}$$

Since the chemical composition of 20Mn2SiV steel is similar to that of the samples we tested, the value of deformation activation energy Q was determined to be 341.97 kJ/mol [27]. According to the strain rate $\dot{\varepsilon}(\dot{\varepsilon} = 5\ s^{-1})$ and the peak stress shown in Table 2, the relationship between $\ln Z$ and $\ln\sigma_p$ (Figure 5) is fitted into linear function, which contributes to achieving the value of A and n, 2.3921×10^{-3} and 8.1387, respectively. Finally, the constitutive equation of the vanadium microalloyed fine grain structural steel pipe can be obtained:

$$Z = \dot{\varepsilon}\exp(341970/RT) = 2.3921\times10^{-3}\sigma_p{}^{8.1387} \tag{3}$$

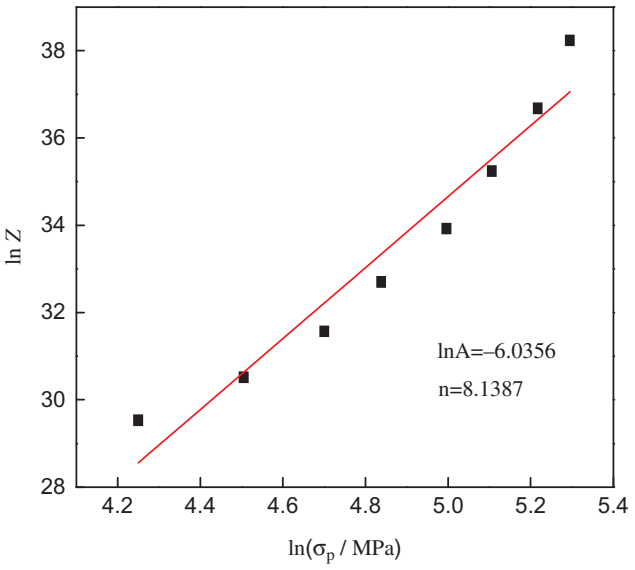

Figure 5: Relationship between $\ln Z$ and $\ln\sigma_p$.

The relationship between critical strain (ε_c), peak strain (ε_p) and Zener-Hollomon Parameters of the vanadium microalloyed cryogenic fine grain structural steel pipe were shown in Figure 6. It can be seen that the critical strain (ε_c) and peak strain (ε_p) of DRX increase with the increasing value of Z. Through regression analysis, the empirical equations are obtained:

$$\varepsilon_c = 3.8616\times10^{-2}Z^{0.0404} \tag{4}$$

$$\varepsilon_p = 3.8722\times10^{-2}Z^{0.0593} \tag{5}$$

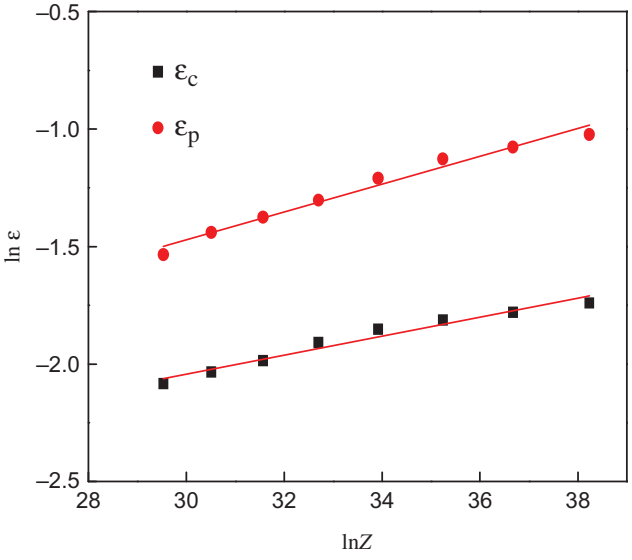

Figure 6: Relationships between critical strain ε_c, peak stain ε_p and Z.

DRX kinetics

Generally, the establishing of DRX kinetics model can quantitatively determine X [18, 26], and the determination of X are derived from the Avrami DRX kinetics equation [26]:

$$X = 1 - \exp\left[-\beta\left(\frac{\varepsilon-\varepsilon_c}{\varepsilon_p}\right)^k\right] \tag{6}$$

where ε is the true strain; ε_c is the critical strain and ε_p is the peak strain of DRX; β and k are the material constants.

In addition, the true stress-strain curves can also give information to calculate the recrystallized fraction, from which the following formula is derived [26]:

$$X = \frac{\sigma_p - \sigma}{\sigma_p - \sigma_c} \tag{7}$$

where σ_c and σ_p are critical stress and peak stress, respectively.

By taking double logarithm from each side of the eq. (6):

$$\ln\ln\left(\frac{1}{1-X}\right) = \ln\beta + k\ln\left(\frac{\varepsilon-\varepsilon_c}{\varepsilon_p}\right) \quad (8)$$

The critical stress (σ_c), the peak stress (σ_p), the critical strain (ε_c) and the peak strain (ε_p) shown in Table 2 into eqs. (6) and (7), the relationship between $\ln\ln(1/(1-X))$ and $\ln((\varepsilon-\varepsilon_c)/\varepsilon_p)$ is almost linear as shown in Figure 7. Through linear regression analysis, the values of β and k are 0.10241 and 1.5567 after calculation, respectively. Afterwards, DRX kinetics model of the vanadium microalloyed fine grain structural steel pipe can be obtained:

$$X = 1 - \exp\left[-0.10241\left(\frac{\varepsilon-\varepsilon_c}{\varepsilon_p}\right)^{1.5567}\right] \quad (9)$$

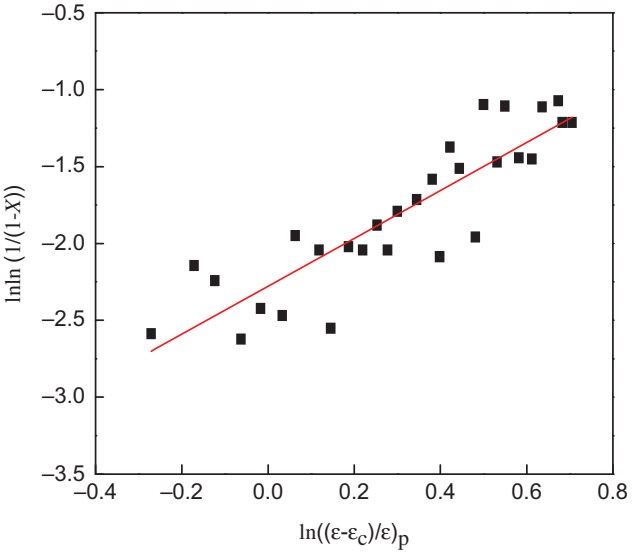

Figure 7: Relationship between $\ln\ln(1/(1-X))$ and $\ln((\varepsilon-\varepsilon_c)/\varepsilon_p)$.

According to the eq. (9) and Table 2, the relationship between the dynamic recrystallized fraction X and true strain ε of the vanadium microalloyed structural steel pipe is presented in Figure 8. It can be seen that the value of X increases quickly after the first slowly with increasing ε at the initial stage of DRX. With further increase in ε, growth rate of the value of X slows down gradually once again till the value of X reaches 1. The ε required for the same amount of recrystallized fractions decreases with increasing deformation temperatures. It can also be found that the theoretical calculation of X would increase from 43.9 % to 100 % as the deformation temperature increasing from 850 °C to 1,050 °C, which is in reasonable agreement with the observation of microstructure, confirming the accuracy of the regression fitting Avrami DRX kinetics.

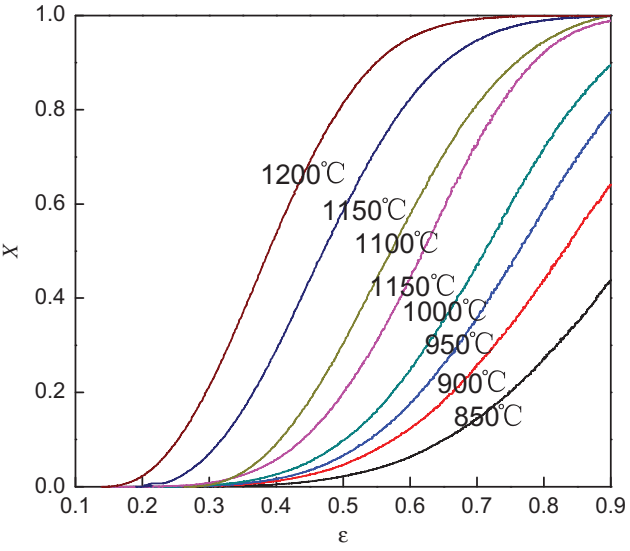

Figure 8: Relationship between X and ε.

The reason accounting for the performance of X can be explained as follows. At the initial stage of DRX, the DRX grains nucleated by means of the bulging of grain boundaries and X increased slowly, which can be ascribed to the low stored distortion energy. With the increasing in ε stored distortion energy increased and the nucleation mechanism had changed into the migration of subgrains and quickly accelerates the process of DRX [28]. Afterwards, deformation grains gradually replaced by fine equiaxed recrystallized grains and the falling stored distortion energy led to a decrease in the driving force of grain boundaries, which accounts for the phenomenon that the increase rate of X becomes slow once again at the later stage of DRX. Moreover, it is well known that the nucleation rate of DRX increased quickly with increasing temperature, and the driving force of DRX in 850–1,000 °C is lower than that in 1,050–1,200 °C, which is mainly contributed to the partially presence of recrystallization microstructure in 850–1,000 °C.

Strain-induced V(C, N) precipitation

High strain rate, firstly, can increase the dislocation density of austenite, leading to an increase in the nucleation sites for precipitates. Secondly, it can shorten the time for the nucleation of precipitates. Prior to studying the strain-induced precipitation behavior of V(C, N) practices at high strain rate and their effective on the DRX, it is essential to determine the solubility temperature of V(C, N). Based on the solubility equations given as follows [29]:

$$\lg[V][C] = 6.72 - 9500/T \quad (10)$$

$$\lg[V][N] = 3.63 - 8700/T \quad (11)$$

where [V], [C] and [N] are their mass fraction in solution and values are 0.14 %, 0.19 %and 0.008 %, separately, in vanadium microalloyed fine grain structure steel pipe. The calculated solubility temperature of VC and VN were 872 °C and 1,049 °C, respectively, which means that VC precipitates are nearly solubilizes in the samples at deformation temperatures. Based on theoretical calculation results, the solubility temperature of V(C, N) is quite closed to VN when precipitation occurs at high temperature [29].

Figure 9 shows the morphology and the particle size distribution of V(C, N) precipitates in samples deformed under temperatures from 850 °C to 1,000 °C. It can be seen that the size of V(C, N) precipitates increases from 5 nm to17 nm while the number is in decrease with increasing temperatures. The statistical of V(C, N) practices is shown in Figure 10, including the number of V(C, N) practices (N_p), the average diameter (D_{ave}), the maximum diameter (D_{max}) and the minimum diameter (D_{min}). Driving force of the precipitation of V(C, N) depends on the degree of supersaturation of V elements in steel and the diffusion ability of V atoms. It is well known that deformation can increase the crystal defects and dislocation density, leading to an increase in the nucleation sites for precipitates [16]. Hence, the number of strain-induced V (C, N) precipitates is higher than that calculated by balance solubility relationships. It is generally believed that the degree of supersaturation of V elements in steel reduces with increasing deformation temperature, which expands the demand of energy fluctuation for the nucleation of V(C, N) practices, and then decelerates the nucleation rates. Furthermore, the diffusion ability of V atoms is strengthened with the increasing temperature, which is beneficial to the growth of V(C, N) practices.

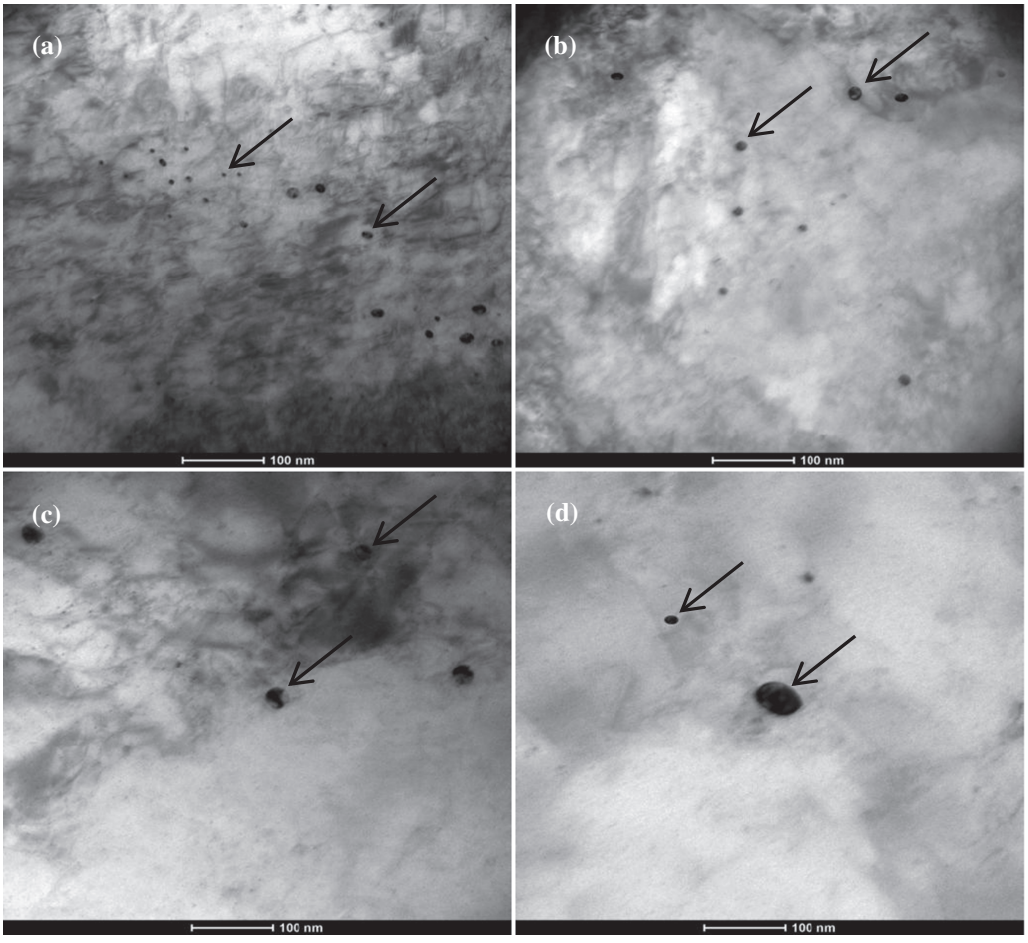

Figure 9: V(C, N) precipitates TEM micrographs of samples deformed under temperatures from 850 °C to 1,000 °C (a) 850 °C (b) 900 °C (c) 950 °C (d) 1,000 °C.

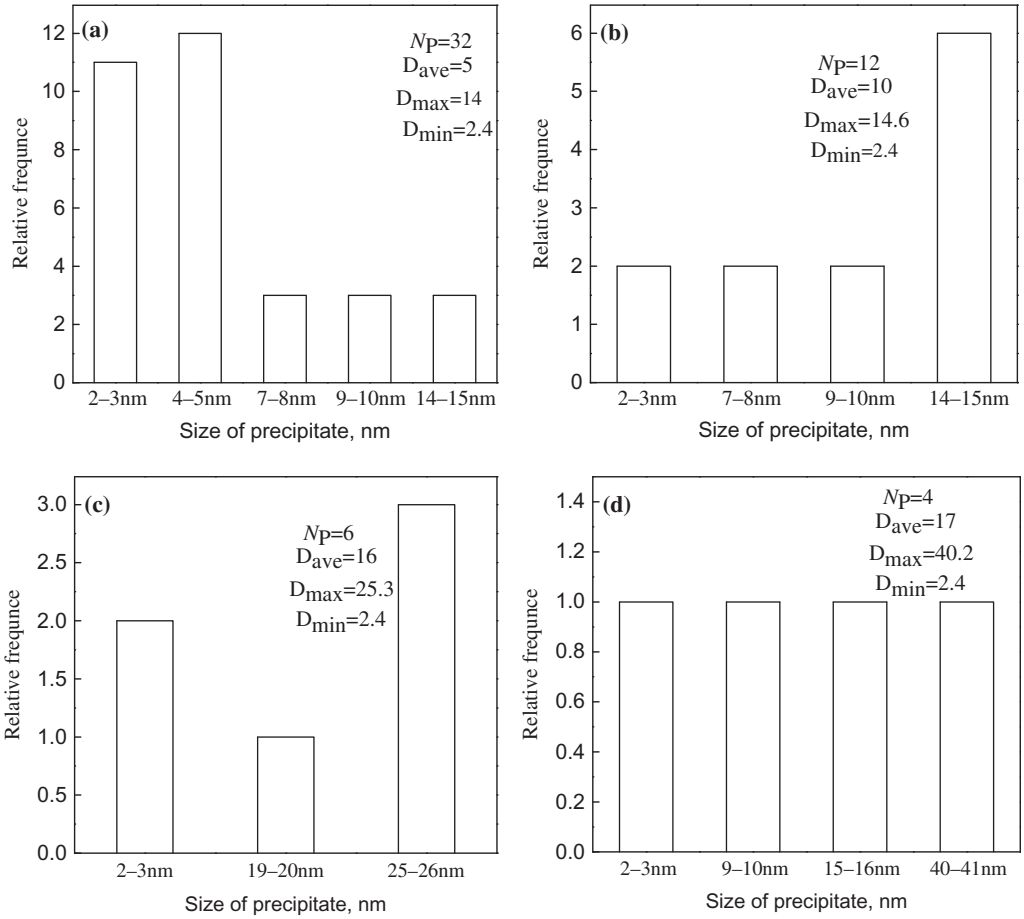

Figure 10: V(C, N) precipitates size distributions of samples deformed under temperatures from 850 °C to 1,000 °C.

This may account for the distribution behavior of V(C, N) precipitates at different deformation temperatures.

According to the recrystallization theory, the driving force of DRX (F_R) can be calculated by [19]:

$$F_R = 0.5\mu b^2 \Delta\rho \tag{12}$$

where μ is the shear modulus (MN/m^2), b is the Burgers vector (m), the value of μ and b for low carbon micro-alloyed steel are 4×10^4 MN/m^2 and 2.5×10^{-10} m, respectively [19]. $\Delta\rho$ is the increase in dislocation density due to deformation (m^{-2}), which is closely related to the factors, such as chemical composition, austenite grain size, and the corresponding deformation conditions. Since the value of $\Delta\rho$ cannot be measured directly, it is normally estimated from the equation proposed by Dutta et al. [14]:

$$\Delta\rho = \left(\frac{\sigma - \sigma_0}{M\alpha\mu b} f_\rho\right)^2 \tag{13}$$

where σ is the flow stress, here we take σ_p as σ; σ_0 is the yield stress corresponding to the strain of 0.02; M is the Taylor factor (3.1 for fcc crystals); α is a constant (0.15); f_ρ is the dislocation density factor that is used to adjust the value of dislocation density under different deformation conditions to obtain the best fit between predictions and experimental observations. According to the empirical value proposed by Dutta et al. [14], f_ρ of 1 is used for the case that the V content is 0.14. Taking both values of σ_p and σ_0 into eq. (13), the calculated values of $\Delta\rho$ are 0.70×10^{15} m^{-2}, 0.58×10^{15} m^{-2}, 0.49×10^{15} m^{-2}, 0.40×10^{15} m^{-2} at deformation temperatures from 850 °C to 1,000 °C, respectively. It is closed to the experimentally measured dislocation density values ($8\pm4\times10^{14}$ m^{-2}) in the subgrain boundary calculated by Rainforth et al. [30] and theoretical deduced critical recrystallization dislocation density values used by Roberts et al. [31], but is lower than values of 4×10^{15} m^{-2} and 1.13×10^{16} m^{-2} used by Burke et al. [32] and Kwon et al. [33], respectively. Finally the driving forces are calculated by means of applying the obtained $\Delta\rho$ values of tested samples to eq. (12), representing 0.88 MN/m^2, 0.73 MN/m^2, 0.62 MN/m^2, 0.51

MN/m^2 at deformation temperatures from 850–1,000 °C, respectively.

Thus, V(C, N) precipitates are located preferentially on subboundaries owning higher dislocation density, and replace part of the grain boundary. Extra energy would be required for the migration of grain-boundary moving away from the particles. The pinning force (F_P) induced by V(C, N) particles can be expressed as [20]:

$$F_P = 4r\gamma N_S \tag{14}$$

where r is the radius of V(C, N) particles; γ is the interface energy per unit area of boundary, taking $\gamma \approx 0.8$ J/m^2 [20]; N_S is the number of V(C, N) particles per unit area of boundary (μm^{-2}). Value of Ns can be estimated from the models, including rigid boundary model, flexible boundary model and sub-boundary model. In the rigid boundary model, the grain boundary is rigid and the distance between grains and precipitates is much farther, which is in good agreement with the experimental results in this paper. Therefore, based on the rigid boundary model, Ns is obtained by [33]:

$$N_S = 3f/2\pi r^2 \tag{15}$$

where f is the average volume fraction of particles, and the value of f can be estimated from the equation proposed by Ebeling et al. [34]:

$$f = \pi N_p \left(D^2 + s^2\right)/6 \tag{16}$$

where D is the diameter of particle (nm); s is the standard deviation of D (nm). Applying eq. (15) and eq. (16) to eq. (14), then the pinning force F_P of DRX can be expressed as follows:

$$F_P = \gamma N_p \left(D^2 + s^2\right)/r \tag{17}$$

Based on the obtained statistics in Figure 10, values of the pinning force F_P under different deformation temperatures from 850 °C to 1,000 °C can be calculated. Table 3 lists the values of pinning forces of V(C, N) precipitates and driving force of dynamic recrystallization under deformation temperatures from 850 °C to 1,000 °C. The results demonstrate that the pinning force of V(C, N) precipitates decreases from 0.61 MN/m^2 to 0.32 MN/m^2 with the temperature increasing from 850 °C to 1,000 °C, which is lower than measured pinning force values (1.46 MPa, 14 MPa) deformed under low strain rate [19, 20], implying that high strain rate do not conductive to the precipitation of V(C, N) particles. The pinning force of V(C, N) precipitates is weak than the driving force of dynamic recrystallization. However, the precipitate-pinning force appears to be of comparable magnitude to the driving force for dynamic recrystallization, which reveals that V(C, N) precipitates could effectively retard rather than prevent the progress of dynamic recrystallization.

Furthermore, the relationship between recrystallization starting time t_s and deformation temperature T may also reflect the effects of alloying elements on DRX. DRX starting time is defined as the ratio of peak strain ε_p and strain rate $\dot{\varepsilon}$: $t_s = \varepsilon_p/\dot{\varepsilon}$ [8]. The relationship between the calculated recrystallization starting time t_s and deformation temperature T is shown in Figure 11. It can be seen that t_s decreases with increasing T, and transition point exists in t_s-T curve at about 1,050 °C, which is consistent with the calculated solubility temperature (1,049 °C) of V(C, N) precipitates. The absolute value of slope in t_s-T curve is smaller as T is lower than 1,050 °C, which means that the extension of recrystallization starting time t_s increases with decreasing temperature. This behavior is also an indicative that the pinning force of strain-induced V(C, N) precipitates did delay the progress of dynamic recrystallization.

Table 3: Pinning forces of V(C, N) precipitates and driving force of DRX of samples deformed under temperatures from 850 °C to 1,000 °C.

T/°C	D, nm	s, nm	N_P, μm^{-2}	F_P, MN/m^2	$\Delta\rho$, m^{-2}	F_R, MN/m^2
850	5	3.6	50	0.61	0.70×10^{15}	0.88
900	10	4.5	19	0.37	0.58×10^{15}	0.73
950	16	10.3	10	0.36	0.49×10^{15}	0.62
1,000	17	14.2	7	0.32	0.40×10^{15}	0.51

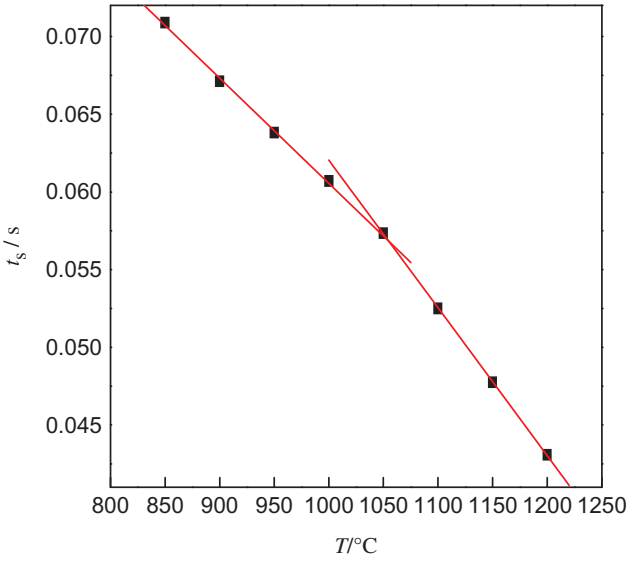

Figure 11: Relationship between recrystallization starting time t_s and deformation temperature T.

Conclusios

(1) The σ-ε curves exhibited no clearly defined stress peaks with typical dynamic recovery behavior and the flow stress increases gradually with the decrease in deformation temperature.

(2) Characteristic points of DRX were accurately determined from the inflection point in strain hardening rate and stress curve, combining with nine polynomial nonlinear fitting. The constitutive equation of the vanadium microalloyed fine grain structural steel pipe is obtained as

$$Z = \dot{\varepsilon}\exp(341970/RT) = 2.3921 \times 10^{-3}\sigma_{\mathrm{p}}{}^{8.1387}.$$

(3) The DRX kinetics model of the vanadium microalloyed fine grain structural steel pipe is established as $X = 1 - \exp[-0.10241(\frac{\varepsilon-\varepsilon_{\mathrm{c}}}{\varepsilon_{\mathrm{p}}})^{1.5567}]$. As the deformation temperature increasing from 850 °C to 1050 °C, the theoretical calculation of X would increase from 43.9 % to 100 %, which is in reasonable agreement with the observation of microstructure, confirming the accuracy of the regression fitting Avrami DRX kinetics.

(4) The calculation pinning force of V(C, N) precipitates is weaken than the recrystallization driving force, revealing that V(C, N) precipitates could effectively retard rather than prevent the progress of dynamic recrystallization. Transition point exists in t_{s}-T curve at about 1,050 °C, further indicating that the pinning force of strain-induced V (C, N) precipitates did delay the progress of dynamic recrystallization.

Funding: This study was financially supported by the Grant from Joint Innovation Fund Project of Jiangsu Province (BY2014003-06), Industrial Technology Innovation Project of Suzhou (SGC201539) and the Priority Academic Program Development of Jiangsu Higher Education Institutions.

References

[1] DIN, E. 10210, Normenausschuß Eisen und Stahl (FES) im DIN Deutsches Institut für Normung eV.
[2] J.H. Kim, S.W. Choi and D.H. Park, Mater. Des., 65 (2015) 914–922.
[3] B. Hwang, Y.M. Kim and S. Lee, Metall. Mater. Trans. A, 36 (2005) 1793–1805.
[4] S. Gündüz and R.C. Cochrane, Mater. Des., 26 (2005) 486–492.
[5] P. Tao, H. Yu, Y. Fan and Y. Fu, Mater. Des., 54 (2014) 914–923.
[6] D.N. Zou, R. Liu and Y. Han, Mater. Sci. Technol., 30 (2014) 411–417.
[7] Y. Cao, H.S. Di and R.D.K. Misra, High Temp. Mater. Processes, 34 (2015) 155–161.
[8] W. Hui, S. Chen and C. Shao, J. Iron Steel Res. Int., 22 (2015) 615–621.
[9] H. Mirzadeh, J.M. Cabrera and J.M. Prado, Mater. Sci. Eng. A, 528 (2011) 3876–3882.
[10] E.I. Poliak and J.J. Jonas, ISIJ Int., 43 (2003) 684–691.
[11] S.H. Cho, K.B. Kang and J.J. Jonas, ISIJ Int., 41 (2001) 63–69.
[12] N.D. Ryan and H.J. McQueen, J. Mater.Process. Technol., 21 (1990) 177–199.
[13] N.D. Ryan and H.J. McQueen, Canadian Metall. Q., 29 (1990) 147–162.
[14] B. Dutta, E.J. Palmiere and C.M. Sellars, Acta Mater., 49 (2001) 785–794.
[15] J.S. Park, Y.S. Ha and S.J. Lee, Metall. Mater. Trans. A, 40 (2009) 560–568.
[16] Z. Wang, X. Mao and Z. Yang, Mater. Sci. Eng. A, 529 (2011) 459–467.
[17] S.F. Medina and C.A. Hernandez, Acta Mater., 44 (1996) 137–148.
[18] H. Wei, G. Liu and X. Xiao, Mater. Sci. Eng. A, 573 (2013) 215–221.
[19] H. Wu, L. Du and X. Liu, J. Mater. Sci. Technol., 27 (2011) 1131–1138.
[20] S.S. Hansen, J.B. Vander Sande and M. Cohen, Metall. Trans. A, 11 (1980) 387–402.
[21] M. Wang, Y. Li and W. Wang, Mater. Des., 45 (2013) 384–392.
[22] A. Najafizadeh and J.J. Jonas, ISIJ Int., 46 (2006) 1679–1684.
[23] C.A.C. Imbert and H.J. McQueen, Mater. Sci. Eng. A, 313 (2001) 88–103.
[24] C.A.C. Imbert and H.J. McQueen, Mater. Sci. Technol., 16 (2000) 532–538.
[25] W. Jin, C. Jun and Z. Zhen, J. Iron Steel Res. Int., 15 (2008) 78–91.
[26] G. Quan, S. Pu and H. Wen, High Temp. Mater. Processes, 34 (2015) 549–561.
[27] M. Spittel and T. Spittel, Steel Symbol/Number: 20MnV6/1.5217[M]//Metal Forming Data of Ferrous Alloys-Deformation Behaviour, Springer, Berlin Heidelberg (2009), pp. 906–911.
[28] E. Brünger, X. Wang and G. Gottstein, Scr. Mater., 38 (1998) 1843–1849.
[29] K. Narita, Trans. Iron Steel Inst. Japan, 15 (1975) 145–152.
[30] W.M. Rainforth, M.P. Black and R.L. Higginson, Acta Mater., 50 (2002) 735–747.
[31] W. Roberts and B. Ahlblom, Acta Metall., 26 (1978) 801–813.
[32] M.G. Burke, L.J. Cuddy and J. Piller, Mater. Sci. Technol., 4 (1988) 113–116.
[33] O. Kwon and A.J. DeArdo, Acta Metall. Mater., 39 (1991) 529–538.
[34] R. Ebeling and M.F. Ashby, Philos.Mag., 13 (1966) 805–834.